

Angular distribution of light scattered from critically quenched liquid mixtures

Y. C. Chou and Walter I. Goldberg

Department of Physics and Astronomy, University of Pittsburgh, Pittsburgh, Pennsylvania 15260

(Received 2 June 1980)

Light scattering was used to determine the structure factor $S(k, \tau)$ of two binary mixtures which were quenched through the critical point. The experiments, which were carried out in isobutyric acid-water and 2,6-lutidine-water, show that the normalized structure factor has the scaling form $\bar{S}(k, \tau) = K^{-3}F(k/K)$ where K^{-1} is the size of a growing domain and $F(x)$ is time independent. Our findings are in approximate agreement with those of Marro *et al.*, who obtained $\bar{S}(k, \tau)$ from a computer simulation of a quenched A - B Ising lattice. The computer experiments yield an initial time dependence in $F(x)$, whereas the light-scattering measurements reveal no evidence of this transient effect over the (dimensionless) time interval $6 \lesssim \tau \lesssim 1000$. The experiments spanned the temperature range $3 \times 10^{-6} \leq \epsilon \leq 2 \times 10^{-5}$, where $\epsilon \equiv |T_f/T_c - 1|$. In this interval the integrated scattering cross section at every instant of time is proportional to $\epsilon^{2\lambda}$ with $0.22 \leq \lambda \leq 0.33$.

I. INTRODUCTION

We have measured the angular distribution of laser light scattered by liquid mixtures which have been quenched into the two-phase region near the critical point. These measurements provide information about the growth rate of nucleating and coalescing domains in the fluid. Our aim was to test a conjecture of Marro, Lebowitz, and Kalos¹ (MLK) that the (normalized) structure function $\bar{S}(k, \tau)$ is of the homogeneous form

$$\bar{S}(k, \tau) = K^{-3}(\tau)F(k/K(\tau)), \quad (1)$$

where $K^{-1}(\tau)$ is a measure of the size of a domain, and where $F(k/K(\tau))$ is independent of time. This same scaling form for the structure factor was first proposed by Binder and Stauffer² and subsequently invoked by Binder *et al.*^{3,4} in theoretical studies of spinodal decomposition.

In the computer simulations of MLK, the structure function was evaluated for an Ising A - B lattice which was quenched (at $\tau = 0$) from an initially disordered state to a temperature and average composition that lay inside the two-phase region. The simulation showed that the time dependence of $F(k/K(\tau))$ disappeared after an initial transient period τ_s . The "settling time" increased as the lattice composition approached its critical value and as the depth of quench decreased.

Though our experiments were carried out on a fluid, which has additional degrees of freedom that are known to influence phase-separation dynamics,^{5,6} Eq. (1) was indeed found to hold. However, no transient behavior was detected, even though the samples were of critical composition and the quench depths were orders of magnitude smaller than in the computer experiments.

Two critical mixtures were studied, isobutyric acid and water (I-W) and 2,6-lutidine and water (L-W). All quenches were carried out in the vic-

inity of the upper critical temperature in I-W and the lower critical temperature in L-W. Thus I-W was driven into the two-phase region by rapid cooling, while the L-W sample was "quenched" by a heating pulse.⁶

The quenches were very shallow in order to take advantage of "critical slowing down";⁷ the final sample temperature T_f never differed from the critical temperatures T_c by more than 9 mK. Under these experimental conditions phase separation could be studied over the interval $6 \lesssim \tau \lesssim 1000$ [see Eq. (6) for a relation between τ and real time t].

To preview our results the reader may wish to glance at Figs. 5 and 6, which show $F(\bar{K})$ vs $\bar{K} \equiv k/k_m(t)$, where k_m is the photon momentum transfer at the angle of maximum scattering. From these graphs it is obvious that Eq. (1) holds very well and that the same function $F(\bar{K})$ characterizes both mixtures.

A partial analysis of our angular distribution measurements in I-W and L-W have been presented in a previous publication by Chou and Goldberg (CG).⁶ In that paper, attention was focused on the time dependence of the maximum in scattering intensity $g(k_m, t)$ and on the collapse rate of the "ring diameter" $k_m(t)$ itself. Whereas MLK found that Eq. (1) was best satisfied when K was taken as the first moment, k_1 , of the structure factor, this parameter will here be identified with k_m . This means we will ignore the evidence from both the computer and laboratory experiments^{1,6} that $k_m^{-1}(t)$ has a somewhat different time dependence than the diameter of a growing cluster and probably k_1^{-1} as well.

The remainder of this paper is organized as follows: Experimental details are presented in Sec. II, and the results in Sec. III. Section IV A contains a comparison between the measurements and the computer simulations of MLK, and brief mention of the theoretical findings of Furukawa⁸ and

Schwartz.⁹ In Sec. IV B our findings will be compared with those of Wong and Knobler,¹⁰ who have also used light scattering to study phase separation in I-W. A reanalysis of their critical-quench data provides a check of Eq. (1) at a single quench depth. This research is summarized in Sec. V.

II. EXPERIMENTAL

The experimental arrangement has been fully described in CG and in an earlier paper by Goldberg *et al.*¹¹ The reader is referred to these references for details.

The I-W and L-W samples were of critical composition and were located in a water bath with a temperature stability of ± 0.1 mK over 1800 sec, which was the duration of the longest run. The cells, which are schematically illustrated in Ref. 11, were reentrant in shape, with an optical path length of only 100 μm to minimize multiple scattering. The critical compositions and temperatures of I-W and L-W are c_c (I-W) = 38.6 wt. % acid, T_c (I-W) = 26.08 $^\circ\text{C}$; (Ref. 12) c_c (L-W) = 28.1 wt. % 2,6-lutidine, T_c (L-W) = 33.37 $^\circ\text{C}$.^{13,14} Two other parameters which will be needed to relate laboratory time t to the dimensionless spin exchange time τ of MLK, are the composition diffusivity D and the correlation length ξ . In the one-phase region they have the following values:

$$D(\text{I-W}) = 2.51 \times 10^{-6} \epsilon^{0.60} \text{ cm}^2/\text{sec} \text{ (Ref. 12)}, \quad (2a)$$

$$\xi(\text{I-W}) = 3.57 \epsilon^{-0.613} \text{ \AA} \text{ (Ref. 14)}, \quad (2b)$$

and

$$D(\text{L-W}) = 0.29 \times 10^{-5} \epsilon^{0.554} \text{ cm}^2/\text{sec} \text{ (Ref. 14)}, \quad (2c)$$

$$\xi(\text{L-W}) = 2.0 \epsilon^{-0.60} \text{ \AA} \text{ (Ref. 14)}. \quad (2d)$$

The light source was the 6328- \AA line (vacuum wavelength) from a He-Ne laser whose output was attenuated to ~ 0.3 mW to prevent local heating of the sample.

Prior to a quench, the sample was permitted to reach thermal equilibrium at a one-phase temperature T_i which was typically several mK from T_c . Variation of $\Delta T_i = |T_i - T_c|$ in the range 1–10 mK produced no observable effects.^{6,11} The L-W mixture was quenched by applying a voltage pulse to a Nichrome heater in the water bath, while in I-W cooling was produced by quickly injecting a few ml of ice water into the bath. With both schemes the final two-phase temperature T_f was reached in ~ 3 sec.

Quenching of the mixture initiated the recording of the angular distribution of the scattered light, $I(\theta, t)$, and the intensity of the unscattered beam,

$I_F(t)$. The origin of time was taken as the instant at which I_F started to decrease precipitously.

To measure $I(\theta, t)$, a rotating mirror arrangement was used to reflect the scattered light into two photodetectors. A minicomputer recorded $I(\theta, t)$, $I_F(t)$, and the background intensity $I_B(\theta)$, which was measured just prior to each quench. Dividing $[I(\theta, t) - I_B(\theta)]$ by $I_F(t)$, to correct for multiple scattering, gave the "corrected intensity,"

$$g(k, t) \equiv g(\theta, t) = [I(\theta, t) - I_B(\theta)] / I_F(t), \quad (3a)$$

where the photon momentum transfer k is related to θ by

$$k = (4\pi n / \lambda_0) \sin(\theta/2). \quad (3b)$$

Here λ_0 is the vacuum wavelength of the source, and n is the refractive index of the mixture.

Treating the mixtures as ideal solutions, one calculates $n(\text{I-W}) = 1.35$ and $n(\text{L-W}) = 1.38$. The validity of the Born approximation is assumed, in which case $g(k, t)$ is proportional to $S(k, t)$.

III. RESULTS

Figures 1 and 2 show typical angular distribution measurements, i.e., $g(k, t)$ vs k at the various times indicated. The quench depths $\Delta T_f \equiv |T_f - T_c|$ were 3.4 mK (I-W) and 0.6 mK (L-W). The solid lines were drawn by eye through the data points. Note that the intensity maximum, $g(k_m, t)$, increases rapidly as the ring collapses,

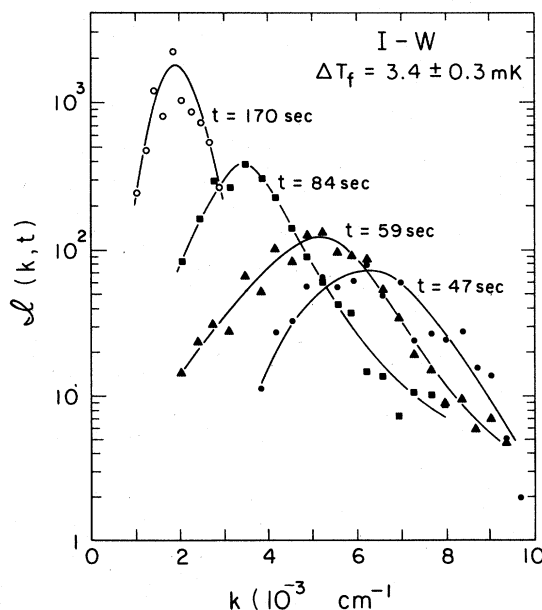


FIG. 1. Scattering intensity $g(k, t)$ versus k at different times in I-W. The quench depth $\Delta T_f = 3.4$ mK.

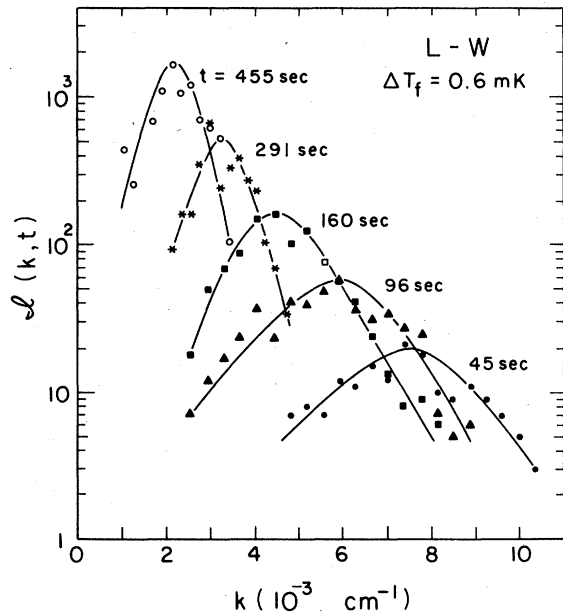


FIG. 2. Scattering intensity in L-W as in Fig. 1 with $\Delta T_f = 0.6$ mK.

i.e., as $k_m(t)$ decreases.

The rather wide scatter in the data points at each t reflects the granular appearance of the scattered light. The size of each speckle is inversely proportional to the diameter of the laser beam and is therefore of little physical interest. The temporal lifetime of these speckles, on the other hand, contains information about the dynamics of phase separation. So far this phenomenon has received little experimental attention^{15, 16} and only recently has been addressed theoretically.¹⁷ Rather, existing theories^{1-4, 8, 9, 18, 19} and computer simulations²⁰ have so far been concerned with the azimuthal average of $S(k, t)$, so that information contained in the lifetime of the spatial fluctuations is averaged out.

The data of Figs. 1 and 2 have been replotted in Figs. 3 and 4 to show $k_m^3(t) g(k, t)$ vs k/k_m . Each set of data points (open squares, closed triangles, etc.) shows an angular distribution at a different t , but all measurements are for a single quench depth, viz., those of Figs. 1 and 2, respectively. Again the solid lines in both figures were drawn by eye through the data points. The scattered intensity is in relative units, but the incident beam did not vary from run to run.

To test Eq. (1) the measurements in Figs. 1-4 were repeated at various quench depths in the range 1 to 5.8 mK in I-W and 0.6 to 1.9 mK in L-W. All the results are summarized in Fig. 5 (I-W) and Fig. 6 (L-W). Here we have plotted the function

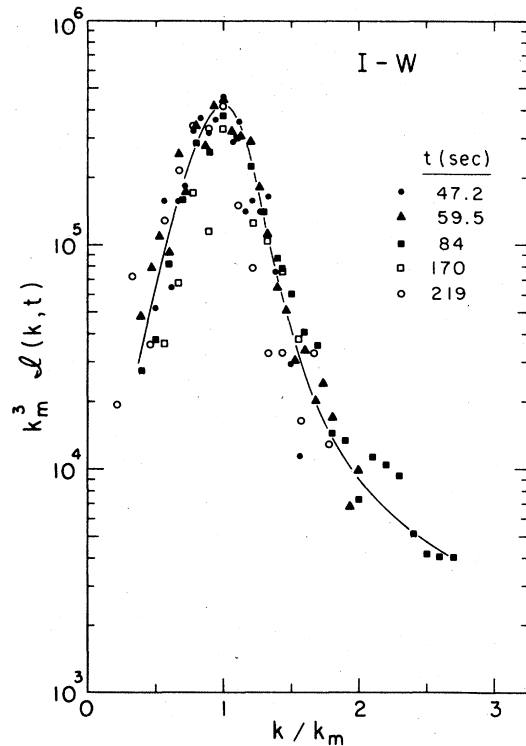


FIG. 3. Unnormalized scaling function $k_m^3 g(k, t)$ versus k/k_m in I-W with the quench depth $\Delta T_f = 3.4$ mK.

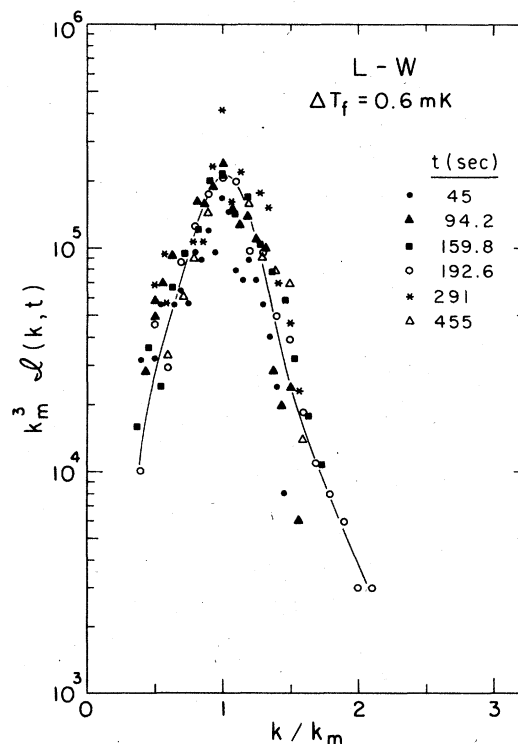


FIG. 4. Unnormalized scaling function $k_m^3 g(k, t)$ versus k/k_m in L-W with the quench depth $\Delta T_f = 0.6$ mK.

$$F(\bar{K}) = k_m^3(t) \bar{g}(\bar{K}, t) \quad (4a)$$

as a function \bar{K} , where the normalized scattering intensity $\bar{g}(\bar{K}, t)$ is defined as

$$\bar{g}(\bar{K}, t) = g(\bar{K}, t) \left(\int_{\bar{K}_a}^{\bar{K}_b} g(\bar{K}, t) \bar{K}^2 d\bar{K} \right)^{-1} \quad (4b)$$

The upper and lower limits on the integral are the maximum and minimum measured values of \bar{K} . They were $\bar{K}_a(\text{I-W}) = 0.5$, $\bar{K}_a(\text{L-W}) = 0.4$, and $\bar{K}_b(\text{I-W}) = \bar{K}_b(\text{L-W}) = 2.0$. Because $g(\bar{K}, t)$ is so sharply peaked at the intermediate value $\bar{K} = 1$, the integral is insensitive to variation of these limits.

The normalization of g removes all adjustable parameters in the function $F(\bar{K})$. These measurements show $F(\bar{K})$ to be independent of time and of quench depth and reveal no appreciable difference between the F functions measured in the two critical mixtures; when Figs. 5 and 6 are superimposed, they are in almost perfect registry.

The measurements in Figs. 5 and 6 constitute a confirmation of Eq. (1) only if multiple scattering is relatively small so that $g(k, t)$ is proportional to the normalized structure function $S(k, t)$ of MLK. While it is difficult to assess the influence of multiple scattering, the best evidence that multiple scattering is not important, comes from the absence of a systematic dependence of $F(\bar{K})$ on quench depth in Figs. 6 and 7. (Multiple scat-

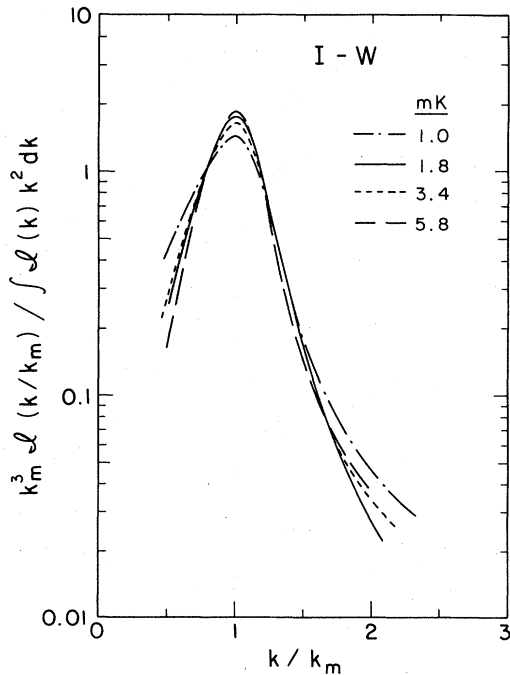


FIG. 5. Normalized scaling function $F(\bar{K})$ versus $\bar{K} = k/k_m$ in I-W at the indicated quench depths.

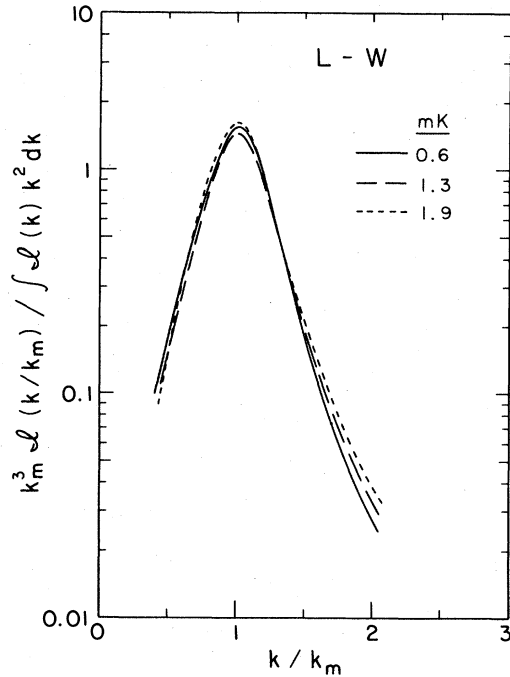


FIG. 6. $F(\bar{K})$ versus \bar{K} in L-W at the three quench depths shown in the figure.

tering is a strongly increasing function of quench depth.) Reference 6 contains a more detailed assessment of the multiple-scattering problem.

An additional limitation of this experiment was

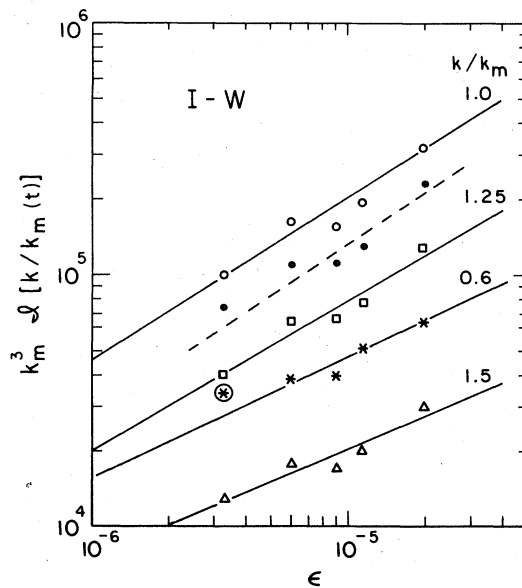


FIG. 7. Unnormalized scaling function $k_m^3 g(k, t)$ versus ϵ in I-W at the four values of \bar{K} indicated on the right. The dashed line is the integral $k_m^3 \int_{0.5}^2 g(\bar{K}, t) d^3 \bar{K}$ versus ϵ .

the parasitic scattering. This background intensity limited the range of wave numbers k_a and k_b over which $g(k, t)$ could be determined. The computer simulations of MLK contain a corresponding limitation on the range of \bar{K} ; in their critical quench runs, the upper and lower bounds on \bar{K} were $\bar{K}_b \approx 5$, $\bar{K}_a = 0.2$. The dimensionless wave number $\bar{K}(t)$ of MLK is the ratio of k to $k_1(t)$ where $k_1(t)$ is the first moment of $S(k, t)$.

Figure 7 is a log-log plot of $k_m^3 g(\bar{K})$ vs $\epsilon \equiv |T_f / T_c - 1|$ in I-W. The solid straight lines are least-squares fits to measurements at four values of \bar{K} in the interval $0.6 \leq \bar{K} \leq 1.25$. All of these lines have approximately the same slope, showing that $g(\bar{K}, t) \propto \epsilon^{2\lambda}$ with $0.22 \leq \lambda \leq 0.33$. The solid circles in this figure show the (time-independent) integral of the angular distribution of the scattered light, $\sigma(\epsilon)$ vs ϵ , where

$$\sigma(\epsilon) = \int_{k_a}^{k_b} g(k, t) k^2 dk. \quad (5)$$

The solid line drawn through these points has a slope $\lambda = 0.30 \pm 0.05$. All the measurements in Fig. 7 suggest that λ is equal to the critical exponent β which describes the shape of the coexistence curve.^{7, 21, 22} The temperature dependence of $\sigma(\epsilon)$ is seen to be entirely different from the scattering which arises from spontaneous fluctuations. As $T \rightarrow T_c$, the latter integral diverges as $\epsilon^{-\gamma}$ ($\gamma \approx 1.25$) rather than approaching zero.

The data in Fig. 7 support a crude model in which closely packed domains, each of volume k_m^{-3} , contribute incoherently to the scattering. In the Born approximation each domain will contribute an intensity proportional to $\langle \Delta c \rangle^2 k_m^{-6}$, so that $g(k, t) \propto \langle \Delta c \rangle^2 k_m^{-3} f(k/k_m)$ where $f(k/k_m)$ is a form factor, and where the miscibility gap $\langle \Delta c \rangle \propto \epsilon^\beta$ is proportional to the electric field scattered by each domain. In CG this model was invoked to explain why the product $k_m^3 \bar{g}(k_m, t) f(1)$ is almost time-independent in I-W and L-W. Those previously published measurements of ring intensity appear again in Fig. 7 on the line labeled $\bar{K} = 1$.

IV. COMPARISON WITH OTHER WORK

A. Computer simulations and theory

The published studies of MLK^{1a} were concerned only with the time evolution of A-B lattices of noncritical composition. However, these authors have extended their calculations to include lattices for which $c = c_c$.^{1b} Again it was found that $S(k, \tau)$ evolved into a scaled form, with the function $F(\bar{K})$ losing its explicit time dependence after a sufficiently long time, τ_s . This settling time was longer for the critical quenches, presumably because diffusion slows down as $T \rightarrow T_c$ [see Eq. (6)

below]. Indeed, they found $\tau_s \approx 3 \times 10^2$ at $\epsilon = 0.41$, whereas $\tau_s \approx 2000$ at $\epsilon = 0.11$.

To compare the results of MLK with experiment one must relate τ to t . For this we take^{6, 23}

$$\tau = (D/\xi^2)t \propto \epsilon^{3\nu} t. \quad (6)$$

With this equation and Eq. (2) our data are calculated to be in the interval $6 \approx \tau \approx 10^3$. Though quench depths in this experiment were four orders of magnitude smaller than those of MLK, there is no evidence of a time lapse before which $F(\bar{K})$ depends on time.

Our measurements will now be compared with the critical-quench computer experiments of MLK.²⁴ At their shallowest quench depth, $\epsilon = 0.11$, $F(\bar{K})$ is maximum at $\bar{K} = \bar{K}_m = 0.8$, with the peak occurring at $F_m \equiv F(\bar{K}_m) = 1.6 \pm 0.2$. The full width of this function at half maximum is $\Delta \bar{K}_{1/2} = 0.7$. Similar values of \bar{K}_m , F_m , and $\Delta \bar{K}_{1/2}$ are obtained in the deeper quenches, $\epsilon = 0.22$ and 0.41 . Figures 5 and 6 yield similar values of these parameters. There it is seen that $\bar{K}_m = 1.0$ in both I-W and L-W, whereas $F_m(\text{I-W}) = 1.6 \pm 0.3$ and $F_m(\text{L-W}) = 1.5 \pm 0.1$. The widths of the peaks are found to be $\Delta \bar{K}_{1/2}(\text{I-W}) = 0.5 \pm 10\%$ and $\Delta \bar{K}_{1/2}(\text{L-W}) = 0.45 \pm 5\%$.

It should be borne in mind that the computer simulations of MLK are not obviously applicable to fluids because the cluster-growth mechanisms are different; the lattice clusters grow by spin exchange, whereas the fluid domains grow by diffusion. This difference in coarsening mechanisms has long been recognized² and has been the subject of subsequent theoretical^{5, 8, 9, 18-20} and experimental^{6, 10} investigations.

Furukawa has also calculated $S(k, \tau)$ starting with Eq. (1), using the diffusive-growth model of Binder and Stauffer² to obtain the average cluster size $K^{-1}(\tau)$. His approach contains approximations that seemingly apply to off-critical quenches only. In any case Ref. 8 does not contain an explicit expression for $F(\bar{K})$. Furukawa's analysis is applicable to a binary fluid mixture, and in fact he compares his results with the off-critical light-scattering measurements of Wong and Knobler.¹⁰

Schwartz⁹ has also observed that $S(k, \tau)$ obeys Eq. (1) for $\tau > 100$. He has obtained a numerical solution to the spinodal decomposition equations of Kawasaki and Ohta¹⁹ and thereby was able to remove some restrictive approximations these authors were required to make. Schwartz finds that $\bar{K}_m = 1.0$ and that $\Delta \bar{K}_{1/2}$ approaches 0.40 when $\tau \geq 100$. Schwartz's analysis is not applicable at very large τ , and in fact he does not carry the calculations of $F(\bar{K})$ past $\tau = 200$.

B. Experiments of Wong and Knobler

We have reanalyzed the critical-quench angular distribution measurements of Wong and Knobler¹⁰ to extract information about $F(\bar{K})$. Figure 3 of that paper shows $I(k, t)$ at a single quench depth, $\Delta T_f = 0.9$ mK ($\epsilon = 3 \times 10^{-6}$), and at five values of t in the interval $t = 36$ sec ($\tau = 5$) and $t = 360$ sec ($\tau = 50$). Their angular distribution measurements spanned the wave-number range $2 \times 10^3 \text{ cm}^{-1} \leq k \leq 9 \times 10^3 \text{ cm}^{-1}$. In reduced units this corresponds to $\bar{K}_a = 0.5$, $\bar{K}_b = 2.0$, as in the present measurements.

The background uncertainty in $I(k, t)$ was sufficiently large that their measurements at $t = 36$ sec could not be included, and at $t = 84$ sec there is uncertainty in the normalization of $g(k, t)$ needed to obtain $\bar{g}(\bar{K}, t)$. Nevertheless, the data in Fig. 3 of WK could be fitted to Eq. (1), yielding a function $F(\bar{K})$ which was qualitatively similar to our own. The main difference was in the measured peak height, F_m . This parameter turned out to be somewhat dependent on t in their measurements. For example $F_m(t = 360 \text{ sec}) \approx 2.7$, whereas $F_m(144 \text{ sec}) \approx F_m(84 \text{ sec}) \approx 1.0$. At $t = 84, 144,$ and 240 sec, their data give $\Delta \bar{K}_{1/2} = 0.7 \pm 0.1$. The difference between the measured F_m in both experiments and the results of MLK, may merely reflect the differing definitions of \bar{K} [recall that we take $\bar{K} = k/k_m$, whereas MLK normalize k by the first moment, k_1 , of $S(k, \tau)$].

V. DISCUSSION AND SUMMARY

We have measured the angular distribution of light scattered from critically quenched mixtures of isobutyric acid and water, and 2,6-lutidine and water. The measurements can be fitted to the scaling form, $g(k, t) = \bar{K}_m^3 F(\bar{K})$, where $\bar{K} = k/k_m(t)$. The scaling function $F(\bar{K})$ is sharply peaked at $\bar{K} = 1$, and is independent of time over the dimensionless interval $6 \lesssim \tau \lesssim 1000$, where τ is related to t by Eq. (6), and is the same in I-W and L-W.

This experiment was motivated by the computer simulations of Marro *et al.*¹ Our findings are similar to theirs, but there are striking differ-

ences. For example, the computer simulations show that $F(k, \tau)$ is initially time dependent, whereas the laboratory experiments give no evidence of this. The computer studies show that this transient behavior disappears after a time τ_s , which increases from 300 to 2000 as the quench depth ϵ decreases from 0.41 to 0.11. A theoretical calculation of Schwartz⁹ also shows $F(\bar{K}, \tau)$ to have an initial time dependence; in his analysis $\tau_s \approx 100$ even very near the critical point. The theory of Schwartz and the work of Kawasaki and Ohta¹⁹ take the fluid degrees of freedom partly into account. It therefore differs from the computer simulations, which produce cluster growth by spin exchange rather than by diffusion.

Putting the laboratory experiments aside there remains the problem of understanding why the spin-exchange model of MLK predicts a much longer settling time than the calculations of Schwartz⁹ and, by implication, the analysis of Kawasaki and Ohta.¹⁹ Perhaps τ_s is reduced by coupling of the composition fluctuations to the velocity field in the fluid. Were this coupling fully taken into account, τ_s might decrease even more.

Phase separation in its initial stage ($\tau \lesssim 10$) appears to be dominated by diffusion, whereas in the late stage ($200 \lesssim \tau \lesssim 1000$), surface-tension effects probably control the rate of domain growth.^{5, 6, 10} As a result, the exponent ϕ which characterizes this rate ($k_m \propto t^{-\phi}$), changes from $\phi \approx \frac{1}{3}$ to $\phi \approx 1$. In spite of a crossover from one growth mechanism to another, there is no corresponding change in $F(\bar{K})$. This is the most surprising result of our experiments.

ACKNOWLEDGMENTS

We have profited from stimulating discussions with K. Binder, D. Jasnow, J. Langer, and A. Schwartz. We also wish to thank J. L. Lebowitz, L. Marro, and M. H. Kalos for providing us with some unpublished results. Our experiments have benefitted greatly from the technical assistance of R. Tobin and J. Zagorac.

¹(a) J. Marro, Joel L. Lebowitz, and M. H. Kalos, *Phys. Rev. Lett.* **43**, 282 (1979); (b) private communication.

²K. Binder and D. Stauffer, *Phys. Rev. Lett.* **33**, 1006 (1974).

³K. Binder, *Phys. Rev. B* **15**, 4425 (1977).

⁴K. Binder, C. Billotet, and P. Miroll, *Z. Phys. B* **30**, 183 (1978).

⁵Eric D. Siggia, *Phys. Rev. A* **20**, 595 (1979).

⁶Y. C. Chou and Walter I. Goldburg, *Phys. Rev. A* **20**, 2105 (1979).

⁷H. E. Stanley, *Introduction to Phase Transitions and Critical Phenomena* (Oxford University, London, 1971).

⁸Hiroshi Furukawa, *Phys. Rev. Lett.* **43**, 136 (1979).

⁹Arthur J. Schwartz (unpublished).

¹⁰Ning-Chih Wong and Charles M. Knobler, *J. Chem. Phys.* **69**, 725 (1978).

¹¹Walter I. Goldburg, Ching-Hao Shaw, John S. Huang, and Michael S. Pilant, *J. Chem. Phys.* **68**, 484 (1978).

¹²B. Chu, F. J. Schoenes, and W. I. Kao, *J. Am. Chem. Soc.* **90**, 3402 (1968); B. Chu, S. P. Lee, and W. T.

- Tscharnuter, Phys. Rev. A 7, 353 (1973).
- ¹³A. Stein, S. J. Davidson, J. C. Allegra, and G. F. Allen, J. Chem. Phys. 56, 6164 (1972).
- ¹⁴E. Gulari, A. F. Collings, R. L. Schmidt, and C. J. Pings, J. Chem. Phys. 56, 6169 (1972).
- ¹⁵M. W. Kim, A. J. Schwartz, and W. I. Goldberg, Phys. Rev. Lett. 41, 657 (1978).
- ¹⁶Walter I. Goldberg, Arthur J. Schwartz, and Mahn Won Kim, Prog. Theor. Phys. Suppl. 64, 477 (1978).
- ¹⁷C. Billotet and K. Binder, Physica 103A, 99 (1980).
- ¹⁸J. S. Langer, M. Bar-on, and H. Miller, Phys. Rev. A 11, 1417 (1975).
- ¹⁹K. Kawasaki and T. Ohta, Prog. Theor. Phys. Jpn. 59, 362 (1978).
- ²⁰A. B. Bortz, M. H. Kalos, J. L. Lebowitz, and M. A. Zendejas, Phys. Rev. B 10, 535 (1974); J. Marro, A. B. Bortz, M. H. Kalos, and J. L. Lebowitz, *ibid.* 12, 2000 (1975); M. Rao, M. H. Kalos, J. L. Lebowitz, and J. Marro, *ibid.* 13, 4328 (1976); A. Sur, J. Lebowitz, J. Marro, and M. Kalos, *ibid.* 15, 3014 (1977).
- ²¹A. Stein and G. F. Allen, J. Phys. Chem. Ref. Data 2, 443 (1973).
- ²²S. C. Greer, Acc. Chem. Res. 11, 427 (1978).
- ²³K. Kawasaki, Ann. Phys. (N.Y.) 61, 1 (1970).
- ²⁴To obtain these parameters, the graphs showing $F(\bar{K})$ vs (\bar{K}) in Ref. 1(b) were renormalized to satisfy Eq. (4).